Supporting Information

Constant Thickness Porous Layer Model for Reaction between Gas and Dense Carbonaceous Materials

Eric A. Morris, Rex Choi, Ti Ouyang, Charles Q. Jia[*]

Department of Chemical Engineering & Applied Chemistry, University of Toronto, 200 College St., Toronto, Ontario, Canada, M5S 3E5

[*]Corresponding author. Tel: +1 416 946 3097. Fax: +1 416 978 8605. E-mail address: cq.jia@utoronto.ca (C.Q. Jia)

1. Sample N_2 Adsorption-Desorption Isotherms

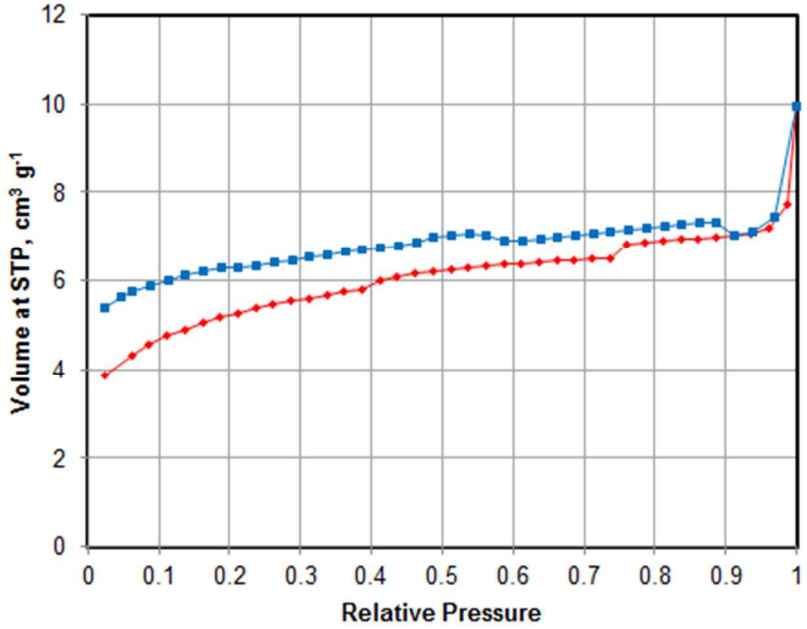

Figure S1. Adsorption (red) / desorption (blue) isotherms for fluid coke, 53–106 µm, before activation. The desorption isotherm was not used in the calculation of physical parameters.

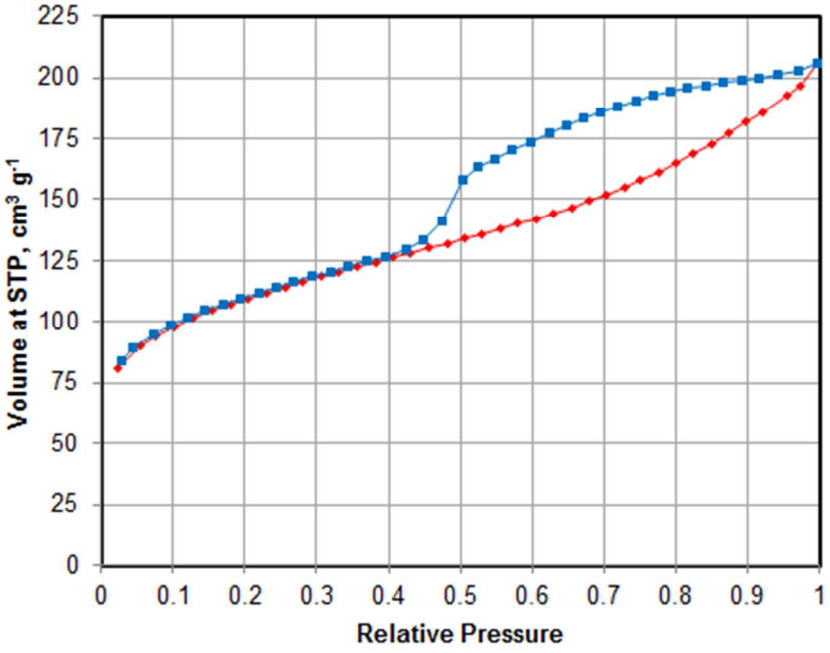

Figure S2. Adsorption (red) / desorption (blue) isotherms for fluid coke, 53–106 µm initial diameter, activated 5 hours at 700°C, 50% SO_2. The desorption isotherm was not used in the calculation of physical parameters, but serves as a qualitative indicator of extensive mesoporosity (as indicated by large hysteresis loop).

2. QSDFT Pore Size Distribution for Raw Coke

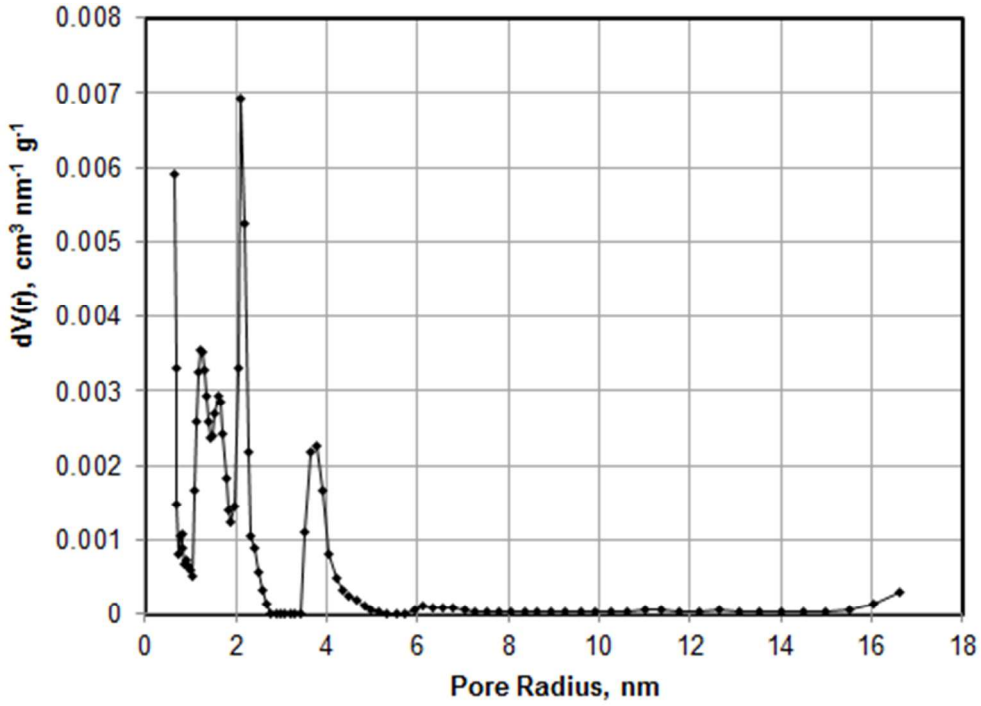

Figure S3. QSDFT pore size distribution for fluid coke, 53–106 μm, before activation. This analysis used only the adsorption branch, assuming slit-shaped geometry for pores less than 1 nm radius, and cylindrical geometry for those greater than 1 nm radius. Note that the initial peak at the far left is an artefact of the limited pressure range; a more extensive micropore analysis at relative pressures down to ~10^{-7} would provide better resolution for pores less than 0.65 nm in radius, although this would entail a much greater analysis time (up to 48 hours).

3. Calculation of Specific Pore Length, L_0

To obtain the total pore length for a range of pore radii, we must integrate under the pore length distribution curve $L(r_P)$. However, most surface analyzers provide the pore volume distribution, $V(r_P)$, as raw output, so we must first convert the data.

For a cylindrical pore, $V = \pi r_P^2 L$, where V is the pore volume, r_P is the pore radius, and L is the pore length. Rearranging to solve for L, we get:

$$L = \frac{V}{\pi r_P^2} \tag{S1}$$

Total pore length is obtained by replacing L and V in Equation S1 with their respective distribution functions and integrating with respect to r_P:

$$\int_0^\infty dL(r_P) = \int_0^\infty \frac{V(r_P)}{\pi r_P^2} dr_P \tag{S2}$$

$$\Rightarrow L = \frac{1}{\pi} \int_0^\infty \frac{V(r_P)}{r_P^2} dr_P \tag{S3}$$

In practice, it is difficult to obtain an analytical expression for $V(r_P)$. Therefore, the $dV(r_P)$ values automatically generated by the Quantachrome ASiQwin software were converted to $dL(r_P)$ using the relations provided above and summed using the trapezoidal rule:

$$Area = 0.5(r_{P,n+1} - r_P)(dL_n + dL_{n+1}) \tag{S4}$$

Where $Area$ denotes the area under the $dL(r_P)$ versus r_P curve between points n and $n+1$. Table S1 provides the software output along with the derived values of $dL(r_P)$ and the trapezoidal area results for unreacted fluid coke, 53–106 μm diameter.

Note that the Random Pore Model requires physical pore dimensions for the unreacted solid material. Thus, in the manuscript, $V(r_P)$, V_P, and L are written as $V_0(r_P)$, V_{P0}, and L_0 to specify them as being initial properties.

Table S1. QSDFT output and L_0 quantification for unreacted fluid coke, 53–106 μm diameter

Pore radius, nm	Pore diameter, nm	Cumulative Pore Volume, $cm^3\ g^{-1}$	dV(r), $cm^3\ nm^{-1}\ g^{-1}$	dL(r), $cm\ nm^{-1}\ g^{-1}$	Area, $cm\ g^{-1}$
0.6495	1.299	4.61E-03	5.91E-03	4.46E+11	1.45E+11
0.678	1.356	4.70E-03	3.31E-03	2.29E+11	9.62E+09
0.708	1.416	4.74E-03	1.48E-03	9.42E+10	4.85E+09
0.739	1.478	4.77E-03	8.15E-04	4.75E+10	2.20E+09
0.7715	1.543	4.80E-03	1.06E-03	5.65E+10	1.69E+09
0.8055	1.611	4.84E-03	1.08E-03	5.32E+10	1.87E+09

0.841	1.682	4.87E-03	8.83E-04	3.97E+10	1.65E+09
0.878	1.756	4.90E-03	6.70E-04	2.77E+10	1.25E+09
0.917	1.834	4.93E-03	7.36E-04	2.79E+10	1.08E+09
0.9575	1.915	4.95E-03	6.41E-04	2.22E+10	1.01E+09
1	2	4.98E-03	5.83E-04	1.86E+10	8.67E+08
1.06032	2.12064	5.01E-03	5.20E-04	1.47E+10	1.00E+09
1.09742	2.19484	5.07E-03	1.68E-03	4.43E+10	1.09E+09
1.13583	2.27166	5.17E-03	2.58E-03	6.37E+10	2.07E+09
1.17559	2.35118	5.30E-03	3.26E-03	7.50E+10	2.76E+09
1.21673	2.43346	5.45E-03	3.56E-03	7.65E+10	3.12E+09
1.25932	2.51864	5.60E-03	3.52E-03	7.07E+10	3.13E+09
1.30339	2.60678	5.74E-03	3.28E-03	6.14E+10	2.91E+09
1.34902	2.69804	5.87E-03	2.94E-03	5.13E+10	2.57E+09
1.39623	2.79246	6.00E-03	2.58E-03	4.21E+10	2.21E+09
1.4451	2.8902	6.11E-03	2.37E-03	3.62E+10	1.91E+09
1.49568	2.99136	6.23E-03	2.40E-03	3.41E+10	1.78E+09
1.54803	3.09606	6.37E-03	2.69E-03	3.57E+10	1.83E+09
1.60221	3.20442	6.53E-03	2.93E-03	3.63E+10	1.95E+09
1.65828	3.31656	6.69E-03	2.84E-03	3.28E+10	1.94E+09
1.71632	3.43264	6.83E-03	2.41E-03	2.60E+10	1.71E+09
1.7764	3.5528	6.94E-03	1.82E-03	1.83E+10	1.33E+09
1.83857	3.67714	7.03E-03	1.38E-03	1.30E+10	9.75E+08
1.90292	3.80584	7.11E-03	1.23E-03	1.08E+10	7.68E+08
1.96952	3.93904	7.20E-03	1.44E-03	1.18E+10	7.55E+08
2.03846	4.07692	7.43E-03	3.30E-03	2.52E+10	1.28E+09
2.1098	4.2196	7.92E-03	6.93E-03	4.96E+10	2.67E+09
2.18365	4.3673	8.31E-03	5.23E-03	3.49E+10	3.12E+09
2.26007	4.52014	8.48E-03	2.19E-03	1.36E+10	1.85E+09
2.33918	4.67836	8.56E-03	1.06E-03	6.14E+09	7.83E+08
2.42104	4.84208	8.63E-03	9.01E-04	4.89E+09	4.52E+08
2.50578	5.01156	8.68E-03	5.58E-04	2.83E+09	3.27E+08
2.5935	5.187	8.71E-03	3.21E-04	1.52E+09	1.91E+08
2.6845	5.369	8.72E-03	1.42E-04	6.26E+08	9.77E+07
2.778	5.556	8.72E-03	0.00E+00	0.00E+00	2.93E+07
2.8755	5.751	8.72E-03	0.00E+00	0.00E+00	0.00E+00
2.976	5.952	8.72E-03	0.00E+00	0.00E+00	0.00E+00
3.08	6.16	8.72E-03	0.00E+00	0.00E+00	0.00E+00
3.188	6.376	8.72E-03	0.00E+00	0.00E+00	0.00E+00
3.2995	6.599	8.72E-03	0.00E+00	0.00E+00	0.00E+00
3.415	6.83	8.72E-03	0.00E+00	0.00E+00	0.00E+00
3.5345	7.069	8.86E-03	1.11E-03	2.84E+09	1.70E+08
3.6585	7.317	9.12E-03	2.17E-03	5.15E+09	4.95E+08
3.7865	7.573	9.41E-03	2.27E-03	5.03E+09	6.52E+08
3.91895	7.8379	9.63E-03	1.66E-03	3.45E+09	5.62E+08
4.0561	8.1122	9.74E-03	8.03E-04	1.55E+09	3.43E+08
4.19805	8.3961	9.81E-03	4.76E-04	8.60E+08	1.71E+08
4.345	8.69	9.86E-03	3.34E-04	5.63E+08	1.05E+08
4.49705	8.9941	9.90E-03	2.44E-04	3.84E+08	7.20E+07
4.65445	9.3089	9.93E-03	1.87E-04	2.75E+08	5.19E+07
4.81735	9.6347	9.94E-03	1.05E-04	1.44E+08	3.41E+07
4.986	9.972	9.96E-03	6.18E-05	7.91E+07	1.88E+07

5.1605	10.321	9.96E-03	3.30E-05	3.95E+07	1.03E+07
5.341	10.682	9.96E-03	0.00E+00	0.00E+00	3.56E+06
5.528	11.056	9.96E-03	0.00E+00	0.00E+00	0.00E+00
5.7215	11.443	9.96E-03	0.00E+00	0.00E+00	0.00E+00
5.9218	11.8436	9.97E-03	4.98E-05	4.52E+07	4.53E+06
6.12905	12.2581	9.99E-03	9.98E-05	8.46E+07	1.35E+07
6.34355	12.6871	1.00E-02	9.01E-05	7.13E+07	1.67E+07
6.5656	13.1312	1.00E-02	8.79E-05	6.49E+07	1.51E+07
6.7954	13.5908	1.00E-02	6.90E-05	4.76E+07	1.29E+07
7.0332	14.0664	1.01E-02	4.68E-05	3.01E+07	9.24E+06
7.2794	14.5588	1.01E-02	3.82E-05	2.30E+07	6.54E+06
7.53415	15.0683	1.01E-02	3.58E-05	2.01E+07	5.48E+06
7.79785	15.5957	1.01E-02	2.60E-05	1.36E+07	4.44E+06
8.0708	16.1416	1.01E-02	2.50E-05	1.22E+07	3.53E+06
8.35325	16.7065	1.01E-02	3.81E-05	1.74E+07	4.18E+06
8.6456	17.2912	1.01E-02	4.14E-05	1.76E+07	5.12E+06
8.9482	17.8964	1.01E-02	3.58E-05	1.43E+07	4.82E+06
9.2614	18.5228	1.01E-02	3.16E-05	1.17E+07	4.07E+06
9.58555	19.1711	1.01E-02	2.41E-05	8.36E+06	3.26E+06
9.92105	19.8421	1.01E-02	2.39E-05	7.73E+06	2.70E+06
10.2683	20.5366	1.02E-02	2.34E-05	7.06E+06	2.57E+06
10.62765	21.2553	1.02E-02	3.79E-05	1.07E+07	3.19E+06
10.99965	21.9993	1.02E-02	5.68E-05	1.49E+07	4.77E+06
11.38465	22.7693	1.02E-02	6.06E-05	1.49E+07	5.74E+06
11.7831	23.5662	1.02E-02	3.89E-05	8.91E+06	4.74E+06
12.1955	24.391	1.02E-02	3.64E-05	7.78E+06	3.44E+06
12.62235	25.2447	1.03E-02	4.56E-05	9.11E+06	3.60E+06
13.0641	26.1282	1.03E-02	4.11E-05	7.67E+06	3.70E+06
13.52135	27.0427	1.03E-02	2.88E-05	5.02E+06	2.90E+06
13.9946	27.9892	1.03E-02	2.80E-05	4.55E+06	2.26E+06
14.48445	28.9689	1.03E-02	1.86E-05	2.82E+06	1.81E+06
14.9914	29.9828	1.03E-02	2.51E-05	3.56E+06	1.62E+06
15.5161	31.0322	1.04E-02	4.66E-05	6.16E+06	2.55E+06
16.05915	32.1183	1.04E-02	1.42E-04	1.76E+07	6.44E+06
16.6212	33.2424	1.06E-02	2.92E-04	3.37E+07	1.44E+07
				Sum:	2.20E+11

The summed result, in units of cm g^{-1}, is then divided by the total pore volume, V_{P0}, to obtain a value in units of cm cm^{-3} (as required by the Random Pore Model). However, as described in Section 2.2 of the manuscript, the total pore volume was calculated using both QSDFT and BJH techniques, since QSDFT is limited to pores less than 33 nm in diameter. Table S2 illustrates how BJH pore size data was appended to the data given in Table S1 as a means of obtaining a more accurate measure of V_{P0}, i.e., 0.0112 cm^3 g^{-1}. This results in a final L_0 value of 2.08×10^{13} cm cm^{-3}, as shown in Table 1 of the manuscript.

Table S2. Use of BJH data for larger pore sizes (BJH data shaded in grey)

Pore radius, nm	Pore diameter, nm	Cumulative Pore Volume, $cm^3\ g^{-1}$
0.6495	1.299	4.61E-03
15.5161	31.0322	1.04E-02
16.05915	32.1183	1.04E-02
16.6212	33.2424	1.06E-02
20.22849	40.45698	1.06E-02
25	50	1.07E-02
43.31692	86.63384	1.08E-02
826.9067	1653.813	1.12E-02

Notes:

- The initial $Area$ value shown in Table S1 is the result of applying the trapezoidal rule between the first data point and the origin, as shown in Figure S4. The result is a rough estimate of the pore length in the small micropore region. Future work would benefit from performing a more detailed micropore analysis, which would allow for more accurate determination of L_0.
- The quantification of L_0 was only carried out in the QSDFT range, i.e., <33 nm. While pores above this size may contribute to pore volume, they will have insignificant impact on overall pore length.

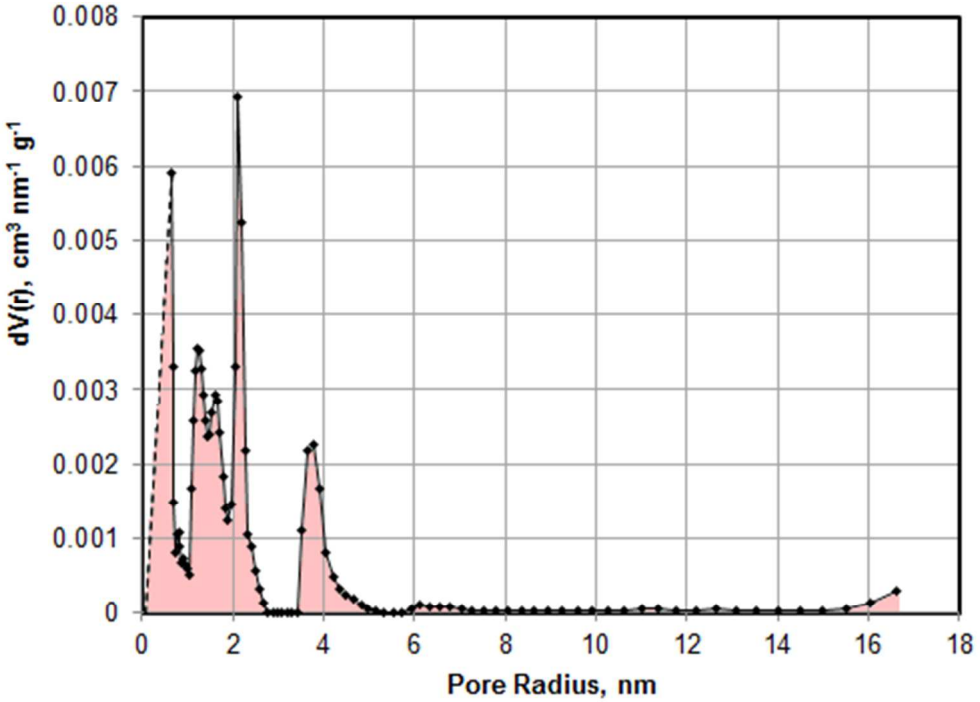

Figure S4. QSDFT pore volume distribution with area used for L_0 determination shaded in pink. The dashed line represents an approximation of the distribution in the small micropore range.

4. Instructions for Simulating Porous Layer Development

Please refer to Figure S5 when reading the following instructions for simulating porous layer development in a fluid coke particle of 12 μm initial diameter using the spherical shell approach.

Column A: Time of activation, which, in this case, is divided into elements of 0.001 hours to enhance resolution.

Column B: R, the outer particle radius based on particle size measurements and following Equation 1.

Column C: r, the unreacted core radius based on SEM core measurements and following Equation 2. Due to the small initial particle size, the value of this column becomes 0 before a constant thickness porous layer, δ_{max}, is achieved (not shown in Figure S5). With larger particle sizes, r would be set to decrease at the same rate as R at the time at which δ_{max} is reached.

Column D: δ, the overall porous layer thickness, or $R - r$.

Column E: $R_{0.05}$, the outer activated radius of the first spherical shell. Since this is the first shell, its outer radius is equivalent to that of the particle, R. The subscript "0.05" refers to the depth of this shell with respect to the initial outer surface, i.e., 0.05 μm. This naming system is, of course, arbitrary. Note that in Figure S5, $R_{0.05}$ is shown in units of μm, whereas, in the manuscript, R_i is defined in units of cm for the sake of consistency within the text.

Column F: $r_{0.05}$, the inner activated radius of the first spherical shell. It follows the unreacted core radius, r, until the point at which the shell reaches its designated thickness of (approximately) 0.05 μm. After this point, $r_{0.05}$ is constant. As with $R_{0.05}$, $r_{0.05}$ is shown in units of μm in Figure S5.

Column G: $\delta_{0.05}$, the activated thickness of the first shell, or $R_{0.05} - r_{0.05}$. This initially increases due to the growing discrepancy between $R_{0.05}$ and $r_{0.05}$, until its designated thickness of (approximately) 0.05 is reached. After this point, it steadily diminishes as R encroaches on the first shell. At some point (row 43, $t = 0.041$ hours, in this case), $\delta_{0.05}$ diminishes to zero, which marks the point at which the other columns related to the first shell must end.

Column H: $X_{0.05}$, the fractional conversion of the first shell. The equation used to calculate X_i is:

$$X_i = \frac{t - t_0}{t_f - t_0}$$

Where t is the current time, t_0 is the time at which the shell initially becomes activated ($t = 0$ for the first shell), and t_f is the time at which the shell is spent ($t = 0.041$ hours for the first shell). This produces a linear progression from 0 to 1.

Column I: $V_{0.05}$, the activated volume of the first shell, as calculated by Equation 7 in the text. In Figure S5, $V_{0.05}$ is shown in units of μm^3.

Column J: $M_{0.05}$, the activated mass of the first shell, as calculated by Equation 8 in the text. This value is displayed in units of grams.

Column K: $S_{0.05}$, the activated surface area of the first shell, as calculated using the Random Pore Model (Equation 3 in the text). It must be noted that, in Figure S5, S_i was calculated in units of $\mu m^2\ \mu m^{-3}$ and subsequently multiplied by V_i (column I), so the values in column K are in units of μm^2.

Column L: $R_{0.1}$, the outer activated radius of the second spherical shell. The starting point for this shell coincides with the point at which the previous shell reaches its designated maximum thickness, since this is the point where r encroaches on the second shell (t = 0.006 hours in Figure S5). Note that $R_{0.1}$ is equal to $r_{0.05}$ until the time at which the first shell is spent (t = 0.041 hours), as this marks the point at which R begins encroaching upon the second shell.

Column M: $r_{0.1}$, the inner activated radius of the second spherical shell. As with the first shell, $r_{0.1}$ is equivalent to r until $\delta_{0.1}$ reaches a thickness of approximately 0.05 μm, after which it remains constant.

Columns N, O, P, Q, and R: Analogous to columns G, H, I, J, and K.

From this point onwards, all remaining shells are constructed in the same manner until the particle has been completely consumed. Total SSA is found by summing all of the S_i columns and dividing by the total mass, as shown in Equation 12 in the text.

Figure S5 may be easier to understand by comparing with Figure 1 in the text. At t = 0.014 hours, the first, second, and third spherical shells have been activated. The activated portion of the first shell is shrinking since it is no longer completely within the porous layer, similar to the 4th shell in Figure 1. The second shell in Figure S5 is completely within the porous layer, as are the 5th, 6th, and 7th shells in Figure 1. The third shell in Figure S5 is not yet completely within the porous layer, and is still growing, similar to the 8th shell in Figure 1. The fourth shell in Figure S5, along with every subsequent shell, is still within the unreacted core and thus is not yet activated (i.e., it does not contribute to total SSA). At t = 0.043 hours, the first shell in Figure S5 is no longer within the porous layer, and, as with the 1st, 2nd, and 3rd shells in Figure 1, is no longer activated.

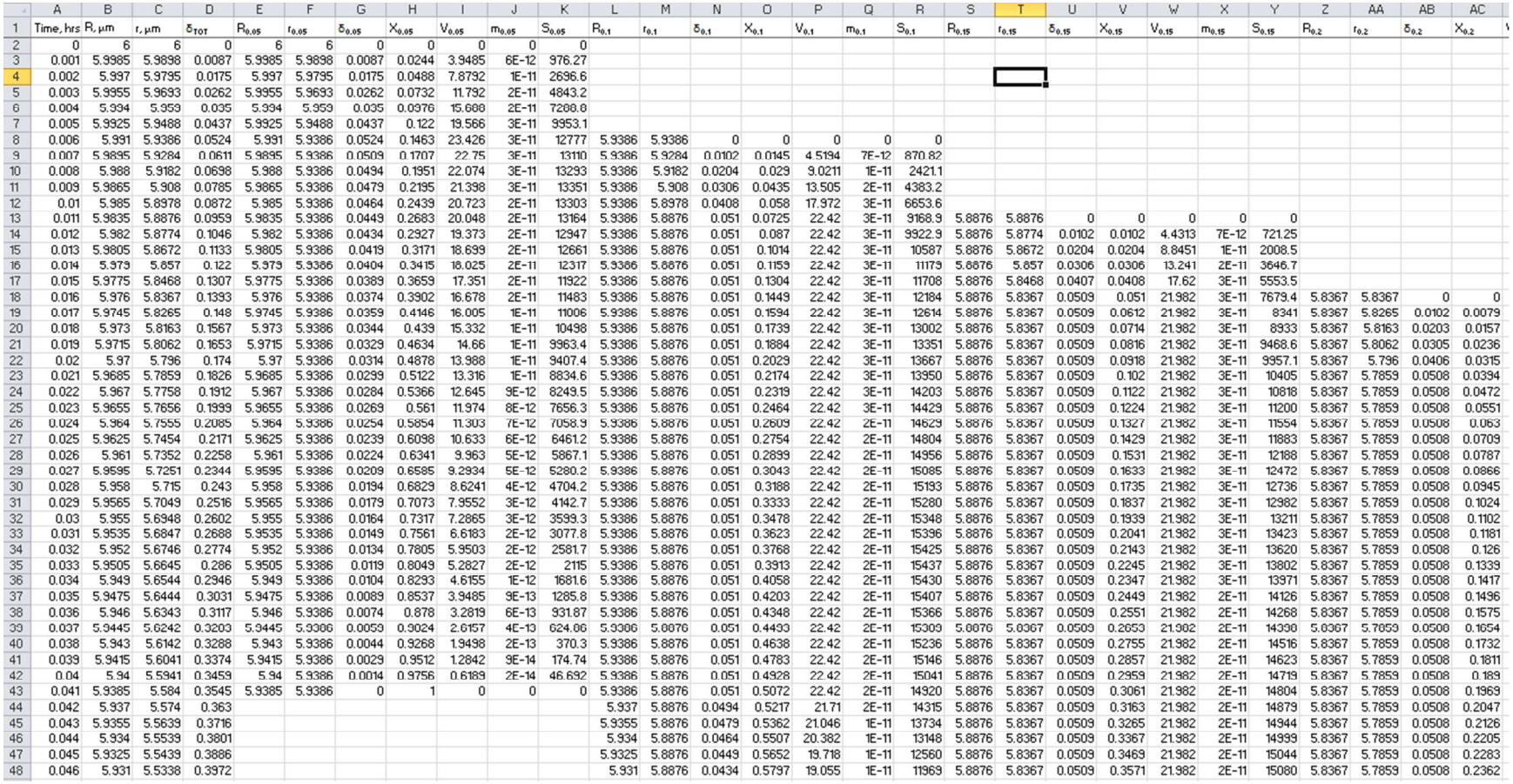

	A	B	C	D	E	F	G	H	I	J	K	L	M	N	O	P	Q	R	S	T	U	V	W	X	Y	Z	AA	AB	AC
1	Time, hrs	R, μm	r, μm	δ_{TOT}	$R_{0.05}$	$r_{0.05}$	$\delta_{0.05}$	$X_{0.05}$	$V_{0.05}$	$m_{0.05}$	$S_{0.05}$	$R_{0.1}$	$r_{0.1}$	$\delta_{0.1}$	$X_{0.1}$	$V_{0.1}$	$m_{0.1}$	$S_{0.1}$	$R_{0.15}$	$r_{0.15}$	$\delta_{0.15}$	$X_{0.15}$	$V_{0.15}$	$m_{0.15}$	$S_{0.15}$	$R_{0.2}$	$r_{0.2}$	$\delta_{0.2}$	$X_{0.2}$	
2	0	6	6	0	6	6	0	0	0	0	0																		
3	0.001	5.9985	5.9898	0.0087	5.9985	5.9898	0.0087	0.0244	3.9485	6E-12	976.27																		
4	0.002	5.997	5.9795	0.0175	5.997	5.9795	0.0175	0.0488	7.8792	1E-11	2636.6																		
5	0.003	5.9955	5.9693	0.0262	5.9955	5.9693	0.0262	0.0732	11.792	2E-11	4843.2																		
6	0.004	5.994	5.959	0.035	5.994	5.959	0.035	0.0976	15.688	2E-11	7288.8																		
7	0.005	5.9925	5.9488	0.0437	5.9925	5.9488	0.0437	0.122	19.566	3E-11	9953.1																		
8	0.006	5.991	5.9386	0.0524	5.991	5.9386	0.0524	0.1463	23.426	3E-11	12777	5.9386	5.9386	0	0	0	0	0											
9	0.007	5.9895	5.9284	0.0611	5.9895	5.9386	0.0509	0.1707	22.75	3E-11	13110	5.9386	5.9284	0.0102	0.0145	4.5194	7E-12	870.82											
10	0.008	5.988	5.9182	0.0698	5.988	5.9386	0.0494	0.1951	22.074	3E-11	13293	5.9386	5.9182	0.0204	0.029	9.0211	1E-11	2421.1											
11	0.009	5.9865	5.908	0.0785	5.9865	5.9386	0.0479	0.2195	21.398	3E-11	13351	5.9386	5.908	0.0306	0.0435	13.505	2E-11	4383.2											
12	0.01	5.985	5.8978	0.0872	5.985	5.9386	0.0464	0.2439	20.723	2E-11	13303	5.9386	5.8978	0.0408	0.058	17.972	3E-11	6653.6											
13	0.011	5.9835	5.8876	0.0959	5.9835	5.9386	0.0449	0.2683	20.048	2E-11	13164	5.9386	5.8876	0.051	0.0725	22.42	3E-11	9168.9	5.8876	5.8876	0	0	0	0	0				
14	0.012	5.982	5.8774	0.1046	5.982	5.9386	0.0434	0.2927	19.373	2E-11	12947	5.9386	5.8876	0.051	0.087	22.42	3E-11	9922.9	5.8876	5.8774	0.0102	0.0102	4.4313	7E-12	721.25				
15	0.013	5.9805	5.8672	0.1133	5.9805	5.9386	0.0419	0.3171	18.699	2E-11	12661	5.9386	5.8876	0.051	0.1014	22.42	3E-11	10587	5.8876	5.8672	0.0204	0.0204	8.8451	1E-11	2008.5				
16	0.014	5.979	5.857	0.122	5.979	5.9386	0.0404	0.3415	18.025	2E-11	12317	5.9386	5.8876	0.051	0.1159	22.42	3E-11	11179	5.8876	5.857	0.0306	0.0306	13.241	2E-11	3646.7				
17	0.015	5.9775	5.8468	0.1307	5.9775	5.9386	0.0389	0.3659	17.351	2E-11	11922	5.9386	5.8876	0.051	0.1304	22.42	3E-11	11708	5.8876	5.8468	0.0407	0.0408	17.62	3E-11	5553.5				
18	0.016	5.976	5.8367	0.1393	5.976	5.9386	0.0374	0.3902	16.678	2E-11	11483	5.9386	5.8876	0.051	0.1449	22.42	3E-11	12184	5.8876	5.8367	0.0509	0.051	21.982	3E-11	7679.4	5.8367	5.8367	0	0
19	0.017	5.9745	5.8265	0.148	5.9745	5.9386	0.0359	0.4146	16.005	1E-11	11006	5.9386	5.8876	0.051	0.1594	22.42	3E-11	12614	5.8876	5.8367	0.0509	0.0612	21.982	3E-11	8341	5.8367	5.8265	0.0102	0.0079
20	0.018	5.973	5.8163	0.1567	5.973	5.9386	0.0344	0.439	15.332	1E-11	10498	5.9386	5.8876	0.051	0.1739	22.42	3E-11	13002	5.8876	5.8367	0.0509	0.0714	21.982	3E-11	8933	5.8367	5.8163	0.0203	0.0157
21	0.019	5.9715	5.8062	0.1653	5.9715	5.9386	0.0329	0.4634	14.66	1E-11	9963.4	5.9386	5.8876	0.051	0.1884	22.42	3E-11	13351	5.8876	5.8367	0.0509	0.0816	21.982	3E-11	9468.6	5.8367	5.8062	0.0305	0.0236
22	0.02	5.97	5.796	0.174	5.97	5.9386	0.0314	0.4878	13.988	1E-11	9407.4	5.9386	5.8876	0.051	0.2029	22.42	3E-11	13667	5.8876	5.8367	0.0509	0.0918	21.982	3E-11	9957.1	5.8367	5.796	0.0406	0.0315
23	0.021	5.9685	5.7859	0.1826	5.9685	5.9386	0.0299	0.5122	13.316	1E-11	8834.6	5.9386	5.8876	0.051	0.2174	22.42	3E-11	13950	5.8876	5.8367	0.0509	0.102	21.982	3E-11	10405	5.8367	5.7859	0.0508	0.0394
24	0.022	5.967	5.7758	0.1912	5.967	5.9386	0.0284	0.5366	12.645	9E-12	8243.5	5.9386	5.8876	0.051	0.2319	22.42	3E-11	14203	5.8876	5.8367	0.0509	0.1122	21.982	3E-11	10818	5.8367	5.7859	0.0508	0.0472
25	0.023	5.9655	5.7656	0.1999	5.9655	5.9386	0.0269	0.561	11.974	8E-12	7656.3	5.9386	5.8876	0.051	0.2464	22.42	3E-11	14429	5.8876	5.8367	0.0509	0.1224	21.982	3E-11	11200	5.8367	5.7859	0.0508	0.0551
26	0.024	5.964	5.7555	0.2085	5.964	5.9386	0.0254	0.5854	11.303	7E-12	7058.9	5.9386	5.8876	0.051	0.2609	22.42	2E-11	14629	5.8876	5.8367	0.0509	0.1327	21.982	3E-11	11554	5.8367	5.7859	0.0508	0.063
27	0.025	5.9625	5.7454	0.2171	5.9625	5.9386	0.0239	0.6098	10.633	6E-12	6461.2	5.9386	5.8876	0.051	0.2754	22.42	2E-11	14804	5.8876	5.8367	0.0509	0.1429	21.982	3E-11	11883	5.8367	5.7859	0.0508	0.0709
28	0.026	5.961	5.7352	0.2258	5.961	5.9386	0.0224	0.6341	9.963	5E-12	5867.1	5.9386	5.8876	0.051	0.2899	22.42	2E-11	14956	5.8876	5.8367	0.0509	0.1531	21.982	3E-11	12188	5.8367	5.7859	0.0508	0.0787
29	0.027	5.9595	5.7251	0.2344	5.9595	5.9386	0.0209	0.6585	9.2934	5E-12	5280.2	5.9386	5.8876	0.051	0.3043	22.42	2E-11	15085	5.8876	5.8367	0.0509	0.1633	21.982	3E-11	12472	5.8367	5.7859	0.0508	0.0866
30	0.028	5.958	5.715	0.243	5.958	5.9386	0.0194	0.6829	8.6241	4E-12	4704.2	5.9386	5.8876	0.051	0.3188	22.42	2E-11	15193	5.8876	5.8367	0.0509	0.1735	21.982	3E-11	12736	5.8367	5.7859	0.0508	0.0945
31	0.029	5.9565	5.7049	0.2516	5.9565	5.9386	0.0179	0.7073	7.9552	3E-12	4142.7	5.9386	5.8876	0.051	0.3333	22.42	2E-11	15280	5.8876	5.8367	0.0509	0.1837	21.982	3E-11	12982	5.8367	5.7859	0.0508	0.1024
32	0.03	5.955	5.6948	0.2602	5.955	5.9386	0.0164	0.7317	7.2865	3E-12	3593.3	5.9386	5.8876	0.051	0.3478	22.42	2E-11	15348	5.8876	5.8367	0.0509	0.1939	21.982	3E-11	13211	5.8367	5.7859	0.0508	0.1102
33	0.031	5.9535	5.6847	0.2688	5.9535	5.9386	0.0149	0.7561	6.6183	2E-12	3077.8	5.9386	5.8876	0.051	0.3623	22.42	2E-11	15396	5.8876	5.8367	0.0509	0.2041	21.982	3E-11	13423	5.8367	5.7859	0.0508	0.1181
34	0.032	5.952	5.6746	0.2774	5.952	5.9386	0.0134	0.7805	5.9503	2E-12	2581.7	5.9386	5.8876	0.051	0.3768	22.42	2E-11	15425	5.8876	5.8367	0.0509	0.2143	21.982	3E-11	13620	5.8367	5.7859	0.0508	0.126
35	0.033	5.9505	5.6645	0.286	5.9505	5.9386	0.0119	0.8049	5.2827	2E-12	2115	5.9386	5.8876	0.051	0.3913	22.42	2E-11	15437	5.8876	5.8367	0.0509	0.2245	21.982	3E-11	13802	5.8367	5.7859	0.0508	0.1339
36	0.034	5.949	5.6544	0.2946	5.949	5.9386	0.0104	0.8293	4.6155	1E-12	1681.6	5.9386	5.8876	0.051	0.4058	22.42	2E-11	15430	5.8876	5.8367	0.0509	0.2347	21.982	3E-11	13971	5.8367	5.7859	0.0508	0.1417
37	0.035	5.9475	5.6444	0.3031	5.9475	5.9386	0.0089	0.8537	3.9485	9E-13	1285.8	5.9386	5.8876	0.051	0.4203	22.42	2E-11	15407	5.8876	5.8367	0.0509	0.2449	21.982	2E-11	14126	5.8367	5.7859	0.0508	0.1496
38	0.036	5.946	5.6343	0.3117	5.946	5.9386	0.0074	0.878	3.2819	6E-13	931.87	5.9386	5.8876	0.051	0.4348	22.42	2E-11	15366	5.8876	5.8367	0.0509	0.2551	21.982	2E-11	14268	5.8367	5.7859	0.0508	0.1575
39	0.037	5.9445	5.6242	0.3203	5.9445	5.9386	0.0059	0.9024	2.6157	4E-13	624.66	5.9386	5.8876	0.051	0.4493	22.42	2E-11	15309	5.8876	5.8367	0.0509	0.2653	21.982	2E-11	14390	5.8367	5.7859	0.0508	0.1654
40	0.038	5.943	5.6142	0.3288	5.943	5.9386	0.0044	0.9268	1.9498	2E-13	370.3	5.9386	5.8876	0.051	0.4638	22.42	2E-11	15236	5.8876	5.8367	0.0509	0.2755	21.982	2E-11	14516	5.8367	5.7859	0.0508	0.1732
41	0.039	5.9415	5.6041	0.3374	5.9415	5.9386	0.0029	0.9512	1.2842	9E-14	174.74	5.9386	5.8876	0.051	0.4783	22.42	2E-11	15146	5.8876	5.8367	0.0509	0.2857	21.982	2E-11	14623	5.8367	5.7859	0.0508	0.1811
42	0.04	5.94	5.5941	0.3459	5.94	5.9386	0.0014	0.9756	0.6189	2E-14	46.692	5.9386	5.8876	0.051	0.4928	22.42	2E-11	15041	5.8876	5.8367	0.0509	0.2959	21.982	2E-11	14719	5.8367	5.7859	0.0508	0.189
43	0.041	5.9385	5.584	0.3545	5.9385	5.9386	0	1	0	0	0	5.9386	5.8876	0.051	0.5072	22.42	2E-11	14920	5.8876	5.8367	0.0509	0.3061	21.982	2E-11	14804	5.8367	5.7859	0.0508	0.1969
44	0.042	5.937	5.574	0.363								5.937	5.8876	0.0494	0.5217	21.71	2E-11	14315	5.8876	5.8367	0.0509	0.3163	21.982	2E-11	14879	5.8367	5.7859	0.0508	0.2047
45	0.043	5.9355	5.5639	0.3716								5.9355	5.8876	0.0479	0.5362	21.046	1E-11	13734	5.8876	5.8367	0.0509	0.3265	21.982	2E-11	14944	5.8367	5.7859	0.0508	0.2126
46	0.044	5.934	5.5539	0.3801								5.934	5.8876	0.0464	0.5507	20.382	1E-11	13148	5.8876	5.8367	0.0509	0.3367	21.982	2E-11	14999	5.8367	5.7859	0.0508	0.2205
47	0.045	5.9325	5.5439	0.3886								5.9325	5.8876	0.0449	0.5652	19.718	1E-11	12560	5.8876	5.8367	0.0509	0.3469	21.982	2E-11	15044	5.8367	5.7859	0.0508	0.2283
48	0.046	5.931	5.5338	0.3972								5.931	5.8876	0.0434	0.5797	19.055	1E-11	11969	5.8876	5.8367	0.0509	0.3571	21.982	2E-11	15080	5.8367	5.7859	0.0508	0.2362

Figure S5. Screenshot from Microsoft Excel illustrating the construction of spherical shells for simulation of porous layer development.